Proceedings of DSCC 2020
ASME 2020 Dynamic Systems and Control Conference
October 4-7, 2020, Pittsburgh Marriott City Center, Pittsburgh, Pennsylvania, USA

DSCC2020-24411

AUTONOMOUS LIGHT ASSESSMENT DRONE FOR DARK SKIES STUDIES

Matthew N. Goodell[1], Takara E. Truong[1], Stephanie R. Marston[1], Brett J. Smiley[1], Elliot R. Befus[1], Alex Bingham[1], Kent Allen[2], Joseph R. Bourne[1], Yi Wei[3], Kate E. Magargal[4], Vellachi Ganesan[3], Daniel L. Mendoza[5], Anil C. Seth[6], Stacy A. Harwood[3], Marc Bodson[2], Tucker Hermans[7] and Kam K. Leang[1, *]

[1]Department of Mech. Engineering & Robotics Center; [2]Department of Electrical & Computer Engineering;
[3]Department of City & Metropolitan Planning; [4]Department of Anthropology;
[5]Department of City & Metropolitan Planning and Atmospheric Sciences;
[6]Department of Physics & Astronomy; [7]School of Computing;
University of Utah, Salt Lake City, Utah 84112.

ABSTRACT

The improper use of artificial light causing skyglow is detrimental to many types of wildlife and can potentially cause irregular human sleeping patterns. Studies have been performed to analyze light pollution on a global scale. However, light pollution data on a local scale is not often available and the effects at local scale have rarely been studied. Herein, a new custom-designed autonomous light assessment drone (ALAD) is described for evaluating light pollution at local scale. The ALAD is designed and equipped with a sky quality meter (SQM) to measure skyglow and a low-cost illuminance sensor to measure light from artificial sources. Outdoor field tests are performed at a remote site in central Utah and the measured results are validated against data from lightpollutionmap.info. The SQM measurements are in agreement with the estimates from the light pollution map, and the initial results demonstrate feasibility of the ALAD for local-scale skyglow assessment.

1 Introduction

Light pollution, illumination of the night sky caused by artificial light, is detrimental to wildlife [1] and has been shown to negatively affect human sleeping patterns [2]. For example, light pollution can change how sea turtles select nesting sites, which can interfere with hatchlings finding the sea once born [3]. Satellite images hold information on the global impact of light pollution and are examined in detail [4]. However, the effect of light pollution on a local scale has not been well studied. Local-scale light information can be used to minimize the impact in select regions, as well as to establish standards for lighting fixtures and allowable emissions.

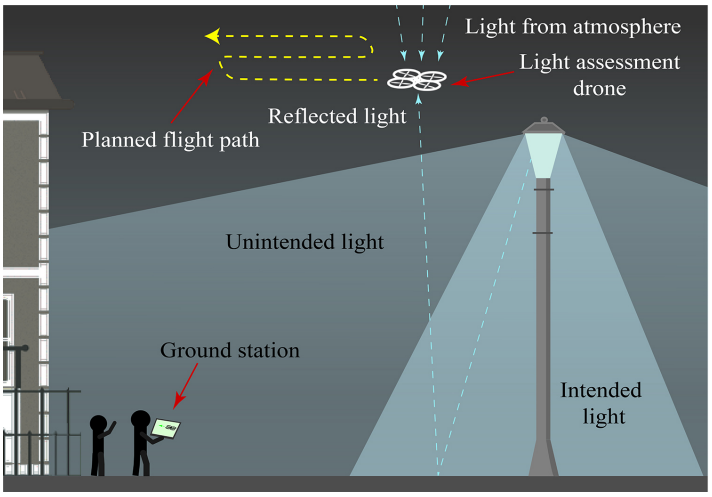

Figure 1: Illustration of how autonomous light assessment drone can be used to gather light pollution data in hard to reach places.

The most advanced method of measuring light pollution at a small scale involves handheld technology, which limits data collection to reachable areas. The contribution of this paper is describing a new way of evaluating light pollution at a local scale using a custom-designed autonomous light assessment drone (ALAD). Figure 1 illustrates the application of the ALAD and how it can be used to gather data that has not been accessible before, such as above light fixtures and in urban environments with buildings and obstructions. The vehicle is designed and equipped with an upward-facing sky quality meter to measure skyglow and a downward low-cost illuminance sensor to measure light from artificial sources.

Little knowledge is available on the effects of light pollution

*†Corresponding author, e-mail: kam.k.leang@utah.edu.

at a local scale. Studies have been performed using satellites to estimate how light pollution affects the planet at a global scale [5]. However, these studies do not show how light pollution varies with height or at a fine geographical level. The proposed ALAD system facilitates gathering light pollution data outside of human reach and at the scale of individual light fixtures. The ALAD system is also designed to be used in classes at the University of Utah to analyze the effects of light pollution as part of a new educational program on Dark Skies Studies. Ultimately, drones like these may also help to reduce the negative effects of new light sources in cities, by identifying those that are not properly configured.

2 Measuring Light Pollution

Two key metrics for measuring light pollution are sky quality (measured in mags/arcsec^2) and illuminance (measured in lux, or lx). These variables are measured with a sky quality meter (SQM) and an illuminance sensor, respectively [6, 7]. The mags/arcsec^2 measurement provides a quantification of sky brightness for a section of the night sky on a logarithmic scale, while illuminance measures luminous flux normal to a surface. While SQM and illuminance data have been collected at the ground level, and some data has been collected and analyzed by satellites at the orbital level [6, 8]. Unfortunately, no data appears to have been collected by near ground aerial vehicles (<400 ft above ground).

Sky quality meters are portable handheld devices that are widely used to measure light pollution [9–11]. The sensor has been used to study the variation of light pollution across different regions [9]. Additionally, SQM measurements have been used to characterize the effects of city light on rural areas [11]. These studies measure sky quality near ground level, but have yet to measure sky quality beyond arms reach.

Multiple studies can be found that measure illuminance for the safety of motorists, cyclists, and pedestrians [12–16]. The illuminance was measured in these studies, but the data was not used to measure the light pollution emanating from light fixtures.

Drones are an increasingly popular platform for remote and novel sensing operations such as autonomous chemical plume localization, field crop phenotyping, and magnetic anomaly detection [17–22]. The remotely-controlled autonomous vehicles are an excellent choice for these applications because they are easy to transport, quick to deploy, and they rapidly collect data over large areas including places that humans cannot easily reach [22]. Additional features such as autonomous flight with data collection and obstacle avoidance can increase quality of data and safety [18, 23]. While the above studies and many others have used drones for remote sensing of various types, none have yet applied drones to measure light pollution.

3 System Design

This section describes the details of the ALAD design. Figure 2 shows the complete vehicle and the key components.

3.1 Drone Platform

A quad-rotor aerial vehicle (quadcopter drone) that serves as the flying-sensor platform was built from scratch using carbon fiber

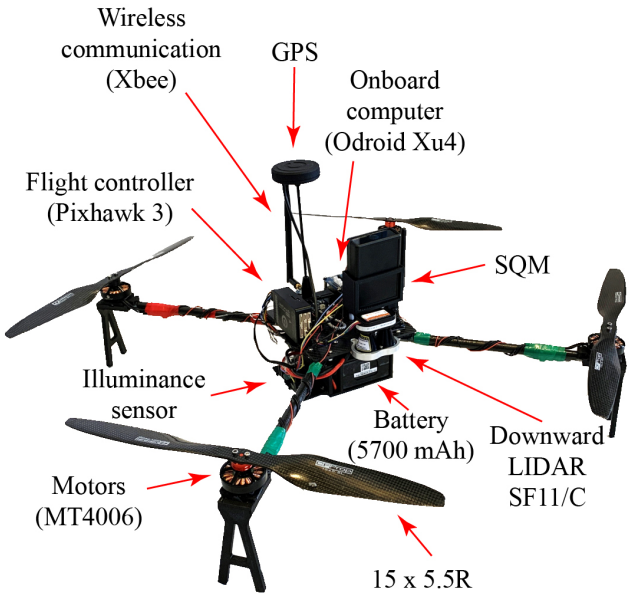

Figure 2: The custom-designed autonomous light assessment drone (ALAD) and highlights of key components.

material for weight reduction. The vehicle carries two on-board light sensors, and it is designed to maximize flight time. The flight controller is a Pixhawk 3 Pro, which interfaces with a Odroid XU4 single board computer (SBC) with an A7 Octa-core CPU and 2GB of LPDDR3. The SBC runs the Robot Operating System (ROS) for motion control, data collection, and mission execution. During operation, for example, desired waypoints are communicated to the SBC which then controls the flight controller for vehicle control and navigation. To communicate with the ground station, two forms of communication were used. The first is a 2.4/5 GHz WiFi module for short-range communication. For long-range communication, a 900 MHz Xbee module is used. To estimate the height relative to local ground, a downward-facing LightWare SF11-C LiDAR is used. The LiDAR unit is not affected by changes in ambient light making it ideal on the ALAD system. The quadcopter is powered by a DJI Tb48s 5.7 Ah Li-Po battery. Power drawn from the SBC is negligible compared to the power consumed by the motors. Propulsion is achieved through four Antigravity 4006 KV380 motors with Tiger 15x5 carbon fiber propellers. The propeller-motor combination results in 3.2 kg of thrust at 50% throttle. With all equipment loaded onto the quadcopter, hover can be sustained for 25 minutes using a single battery pack.

3.2 Light Sensing

Two light sensors are mounted on the ALAD to measure light pollution: a Unihedron sky quality meter and a low-cost Texas Instruments OPT3001 illuminance sensor. The SQM measured sky brightness, recorded in magnitudes per square arcsecond (mags/arcsec^2). The magnitude is calculated by

$$m_1 = -2.5\log_{10}(F) + m_2, \quad (1)$$

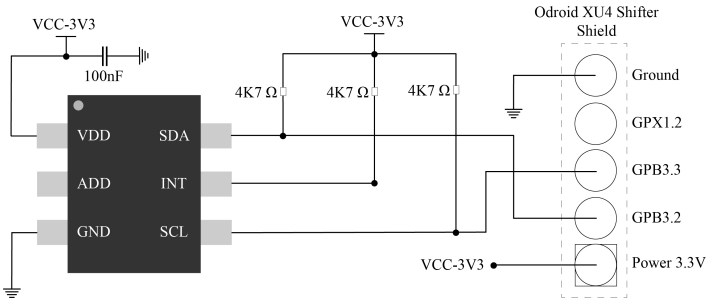

Figure 3: Wiring diagram for the low-cost TI OPT3001 illuminance sensor to the Odroid XU4 SBC shifter shield.

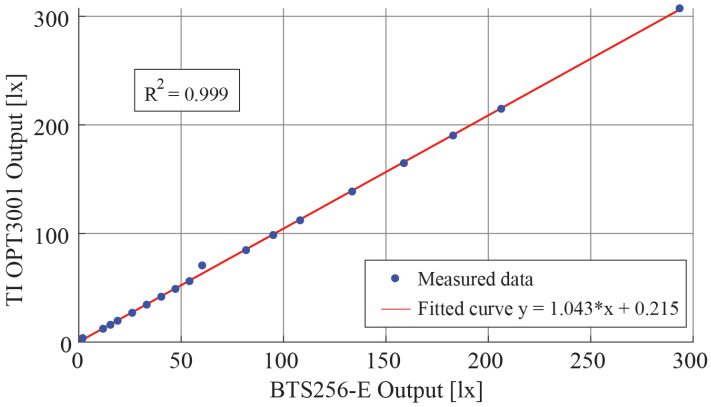

Figure 4: Calibration of the TI OPT3001 illuminance sensor using a BTS256-E light meter.

where m_1 is the magnitude, F is the intensity of the light source, and m_2 is a reference magnitude calibrated by the manufacturer. A change in 0.1 mags results in roughly a 10% change in flux, while a change of 5 mags results in a change of 100 in flux. This is the preferred way of measuring light pollution by astronomers.

The SQM was factory calibrated. The greater the light shining on the SQM, the smaller the measurement. An average reading of a sidewalk lit at night is around 14 mags/arcsec^2. A reading of 21 or higher means almost no light pollution [24]. The frequency of the readings ranged from 0 Hz to 50 Hz and is dependent on the amount of light hitting the sensor. The SQM sent data measurements through USB communication when the ALAD is at the pre-specified waypoints during operation.

The downward facing low-cost TI OPT3001 illuminance sensor measures only visible light from all light sources. The range of measurement spans from 0.01 lx up to 83,000 lx. The sensor can be sampled at 100 milliseconds or 800 milliseconds. The lower sampling rate increases the accuracy of the readings at lower light levels. The sensor communicates with the Odroid SBC through an I^{2}C link, as shown in Fig. 3, and the data is recorded at the specified waypoints. The illuminance sensor accuracy was validated through the use of a BTS256-E Luxmeter. Validation results are shown in Fig. 4. A preliminary flight test was performed at night under an LED lamp and at the start of a trailhead where there was very little light. The illuminance data from the flight test are shown in Fig. 5.

3.3 Ground Station and Software Architecture

A laptop computer running custom-designed software serves as the ground station to control and launch the ALAD. The

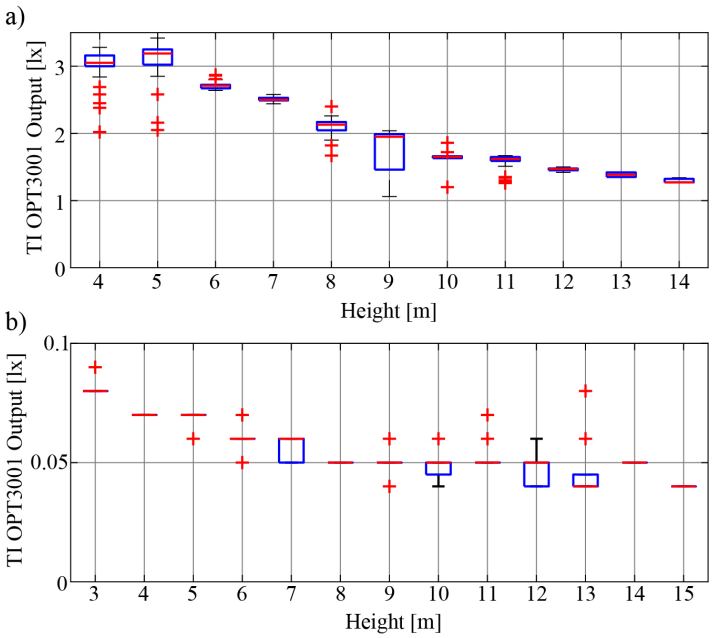

Figure 5: Preliminary results from TI OPT3001 illuminance sensor mounted to the ALAD: (a) illuminance data underneath an LED lamp, (b) illuminance data at the start of a trailhead with no direct light sources.

software, hardware, and communication architecture is shown in Fig. 6, and the arrows in the figure represents the flow of information between various nodes. Waypoint lists and execution commands are sent to the ALAD. ALAD status and navigation data are sent back to the ground station.

An example of the custom GUI is shown in Fig. 7, illustrating the key features of the software package. The ground station allows users to select the mission types (*i.e.*, waypoint missions or raster scans), start the mission/test, and send control commands to the ALAD. Once the ALAD receives start flight command, it is completely independent of the ground station and operates autonomously. If the ALAD went out of range from the ground station's communication, it is programmed to complete its mission independently from the ground station. Refer to [17] for information about the ALAD autonomous navigation system.

4 Measurement Modes

The ALAD operates in two different measurement modes: (1) manual-waypoint and (2) raster-scan mode. In manual-waypoint mode, measurements are made at specific locations set by the user. In raster-scanning mode, a selected area is autonomously scanned and data is gathered at distributed locations. The results presented herein are focused on specific waypoints directly overhead of light posts which have been chosen by the user. The ALAD was programmed to collect SQM and illuminance data at each waypoint. The data consisted of time-stamped illuminance data, GPS coordinates, and altitude measurements from the onboard LiDAR range sensor.

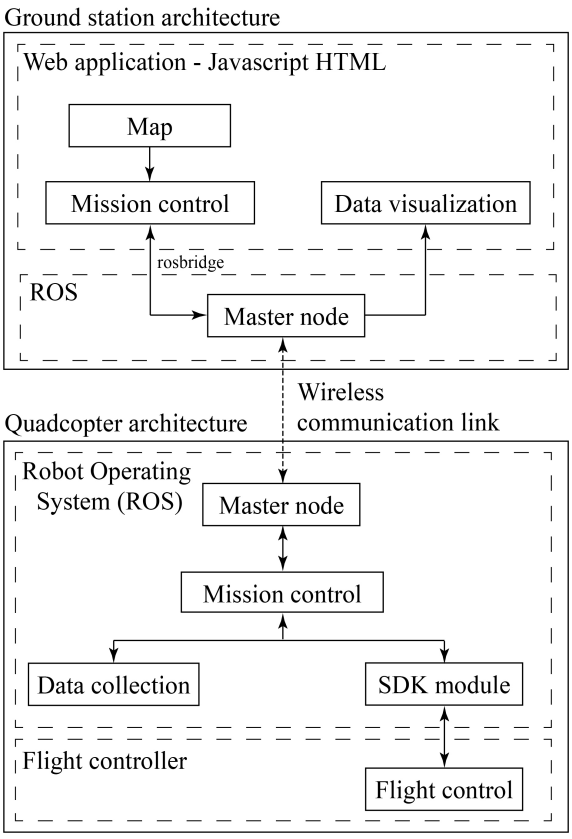

Figure 6: Software, hardware, and communication architecture. Arrows represents the flow of information between various nodes.

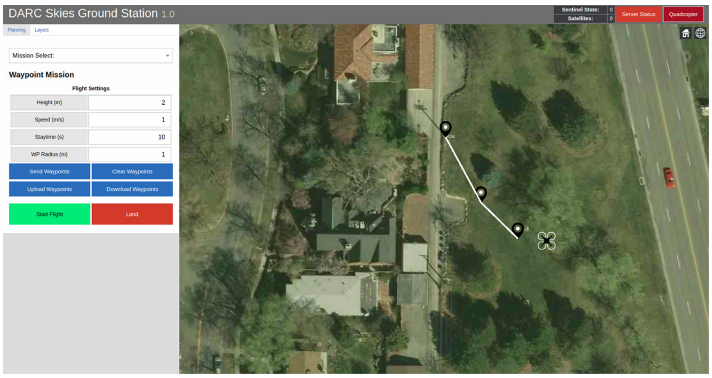

Figure 7: Custom-designed GUI for selecting mission types, specifying waypoints, and real-time location information of the ALAD.

5 Outdoor Field Experiments and Results

To demonstrate feasibility of the ALAD system, light assessment experiments were conducted in the town of Helper, Utah, where the town has a population of around 2,000 [25]. Helper was selected because of its small size and its ranking as a class 4 site on the Bortle scale (mildly polluted rural and suburban areas). Tests were performed in dark environments and above different types of light fixtures and the light SQM and illuminance data were recorded. Full-scale experiments were conducted to determine which light sources (specifically lampposts) were emitting the most light, and therefore contributing the most to light pollution. The experiment was performed on Friday, February 20th, 2020 when the moon was in its third-quarter close to a new moon. As the city of Helper has been working towards a Dark Skies certification, their mayor was interested in determining how to reduce light pollution. The full-scale test included performing sensor readings in two areas: the parking lot of a cemetery and Main Street.

The cemetery parking lot was determined to have only one light source, making it an almost entirely dark area, allowing for data to be collected over a lamppost that was unaffected by any other light source. Main Street was determined to be well-lit with various models of lampposts, allowing for data to be collected on the light emitted from different types of lampposts. Both flight tests were performed after astronomical dusk to ensure completely dark skies.

For the first test at the cemetery, the ALAD was initially flown at altitudes of 2 meters and 10 meters in the parking lot, away from the shielded lamppost, to record sensor data in near-total darkness. It was then flown directly over the lamppost at an altitude of 10 meters and 15 meters to determine the amount of light being emitted into the sky shown (see Fig. 8). The TI OPT3001 illuminance and SQM sensor readings can be seen in Fig. 9.

The TI OPT3001 illuminance sensor data, as seen in Fig. 9, shows illuminance values that follow expectations at the Cemetery. For the 2 and 10 meter flights in the dark parking lot, the recorded values came out to be 0.08 and 0.03 *(lx)*. There is little variation in these two values, as is expected in an almost completely dark area. For the 10 and 15 meter flights over the shielded lamppost, the recorded values were 1.13 and 0.95 *(lx)*.

The SQM sensor data is presented in Fig. 9. For the 2 and 10 meter flights in the dark parking lot, the recorded values came out to be 20.85 and 20.86 mags/arcsec^2. Again, as might be expected in a very dark area, there is little variation in recorded values at different heights. These values also fall in class 4 on the Bortle scale Fig. 11, which represents the transition between rural and suburban environments. For the 10 and 15 meter flights over the shielded lamppost, the recorded values were 20.57 and 20.68 mags/arcsec^2. These values also fall in class 4, which is consistent with a measurement above a shielded light source.

For the second test on Main Street, the ALAD was flown in the center of the road at a low altitude of 3 meters, then at a high altitude of 15 meters (above the surrounding lampposts). Multiple tests were performed here where the ALAD moved down Main Street so that it was positioned in-between both LED and sodium-vapor (SV) lampposts. For this test, TI OPT3001 illuminance and SQM sensor readings are shown in Fig. 9.

The TI OPT3001 illuminance sensor data, as seen in Fig. 9, shows illuminance values that fit expectations for Main Street. The three flights over LED lampposts for the 3 and 10 meter flights were averaged, and the values came out to be 1.61 and 1.79 lx. The sodium-vapor (SV) lamppost values recorded were 2.71 and 1.89 lx. These values fall within the expected range: as the sensor was facing downwards, the data at 3 meters was expected to be lower than the data collected above the light sources at 10 meters. The values are within a range that is to be expected for an urban street at night.

The SQM sensor data, as shown in Fig. 9, shows very reason-

Figure 8: Photographs of team conducting experiments in Helper, Utah. Top left shows ALAD measuring light pollution above a single light post near town cemetery and top right shows experiments on Main Street of Helper.

able readings on Main Street. The averaged three flights over the shielded LED lampposts at 3 and 10 meters came out to 16.59 and 20.26 mags/arcsec^2, and the sodium-vapor (SV) lamppost values were 13.88 and 20.83 mags/arcsec^2. For the 3-meter height tests, the values for the LED and SV lights both fall in class 8-9 on the Bortle scale Fig. 11, which represents a city sky. This result is consistent for data recorded under the light sources, resulting in direct exposure to the lights. For the 10-meter height tests, the values fall in class 5 and class 4 on the Bortle scale, which represents the transition between rural and suburban environments. These values

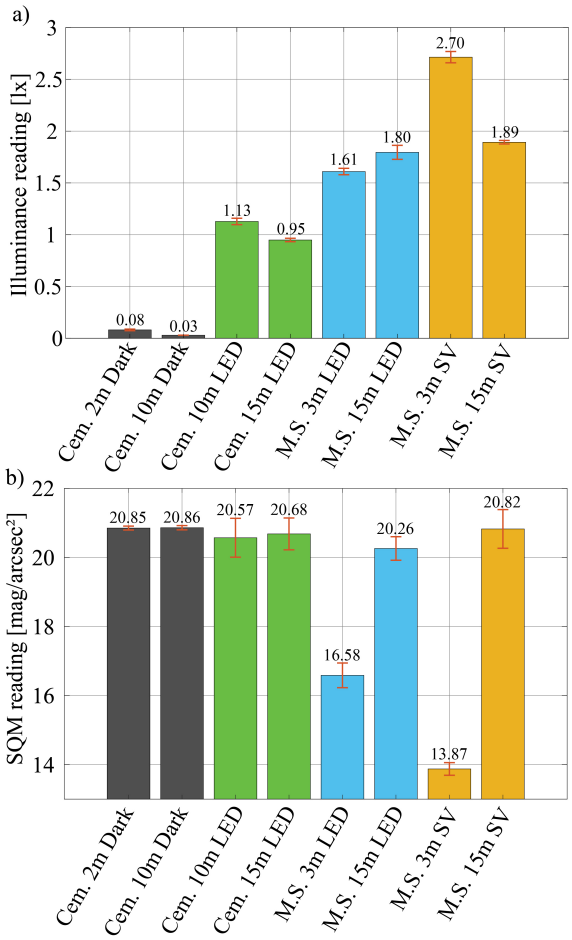

Figure 9: (a) Mean illuminance sensor and (b) Mean SQM data. Red bars indicate 95% confidence interval; black and green are cemetery readings in complete darkness and above a light post, blue and yellow are LED and low-pressure sodium vapor light posts. Data taken on Main Street.

are expected as SQM values are higher (less light pollution) above a shielded light source. The SV light is brighter than the LED when underneath the lamppost, but darker when above; thus, the SV lampposts appear to contribute less light pollution as expected due to reduced atmospheric scattering at longer wavelengths.

6 Discussion

This paper explored the application of an aerial vehicle to analyze light pollution vertically outside the reach of traditional handheld instruments. A field test was performed in Helper, Utah, to analyze the effects of light pollution from various lampposts. As a result, the LED lampposts were shown to have lower illuminance and SQM effects on the surrounding environment compared to the sodium vapor lamp post.

Exploring light pollution on a local scale is not only important to minimize the amount of light being emitted into the sky, but also to reduce its negative impacts on wildlife and human sleeping patterns. Figure 10 shows the intensities of light pollution across the United States, estimated from satellite data, and Fig. 11 shows

various locations ranked by their SQM value and Bortle scale measurement.

Future experiments are planned to model the effects of light pollution in three-dimensional space, as well as with a camera to take raw photos and analyze the spectral intensity of light sources. Physical experiments can also be conducted that test different light fixture designs and light source combinations.

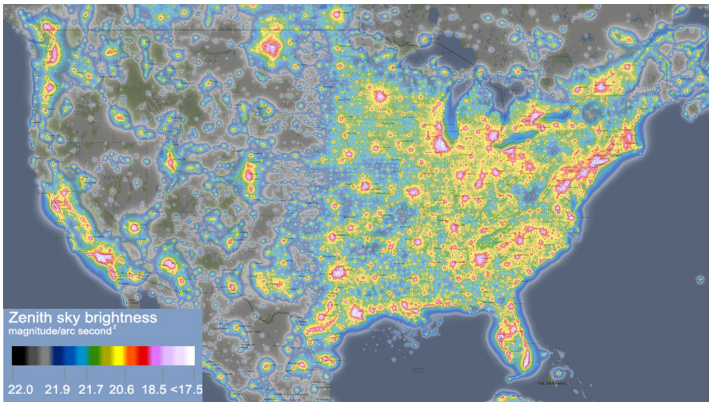

Figure 10: Zenith sky brightness across the United States showing estimated SQM readings in $mags/arcsec^2$ [26]. SQM data is estimated through satellites measuring light which has escaped into the atmosphere.

7 Conclusions and Future Work

This paper describes the design of an autonomous light-assessment aerial robot for dark skies studies. The system enables light pollution data to be collected at a local scale and at various heights, which has not been available until now. The platform was equipped with an SQM to measure reflected light and with an illuminance sensor to measure direct light from specific sources. Results were presented to demonstrate proof-of-concept. Future work includes gathering SQM data at additional locations and creating models of light pollution in three-dimensional space. Methods will also be deduced to improve sky quality metrics, which will contribute to quality of life as well as enhancing tourism for certain locations.

8 Acknowledgements

The authors acknowledge the financial support of the W.M. Keck Foundation. Any opinions, findings, and conclusions or recommendations expressed in this material are those of the authors and do not necessarily reflect the views of the Keck Foundation. Authors also thank John Barentine, Bryan Boulanger, Stephen Goldsmith and David B. Kieda for their valuable input on the project.

REFERENCES

[1] T. Raap, R. Pinxten, and M. Eens, "Light pollution disrupts sleep in free-living animals," *Scientific Reports*, vol. 5, no. 1, pp. 1–8, 2015.

[2] Y. S. Koo, J.-Y. Song, E.-Y. Joo, H.-J. Lee, E. Lee, S. kun Lee, and K.-Y. Jung, "Outdoor artificial light at night, obesity, and sleep health: Cross-sectional analysis in the koges study," *Chronobiology International*, vol. 33, no. 3, pp. 301–314, 2016.

[3] B. E. Witherington and R. E. Martin, "Understanding, assessing, and resolving light-pollution problems on sea turtle nesting beaches," Florida Marine Research Institute, Tech. Rep. TR-2, 2000.

[4] F. Falchi, P. Cinzano, D. Duriscoe, C. C. M. Kyba, C. D. Elvidge, K. Baugh, B. A. Portnov, N. A. Rybnikova, and R. Furgoni, "The new world atlas of artificial night sky brightness," *Science Advances*, vol. 2, no. 6, 2016.

[5] J. Bennie, T. Davies, J. Duffy, R. Inger, and K. Gaston, "Contrasting trends in light pollution across Europe based on satellite observed night time lights," *Scientific Reports*, vol. 4, p. 3789, 01 2014.

[6] A. G. Admiranto, R. Priyatikanto, S. Maryam, Ellyyani, and N. Suryana, "Preliminary report of light pollution in indonesia based on sky quality observation," *Journal of Physics: Conference Series*, vol. 1231, p. 012017, May 2019.

[7] S. Hideaki, "Research on light pollution by using a sky quality meter," *Young Scientists Journal*, vol. 6, no. 13, p. 23, 2013.

[8] M. J. Butt, "Estimation of light pollution using satellite remote sensing and geographic information system techniques," *GIScience & Remote Sensing*, vol. 49, no. 4, pp. 609–621, 2012.

[9] C. Pun and C. So, "Night-sky brightness monitoring in hong kong," *Environmental Monitoring and Assessment*, vol. 184, no. 4, pp. 2537–2557, 2012.

[10] M. Kocifaj, T. Posch, and H. A. Solano Lamphar, "On the relation between zenith sky brightness and horizontal illuminance," *Monthly Notices of the Royal Astronomical Society*, vol. 446, no. 3, pp. 2895–2901, 11 2014.

[11] A. Jechow, F. Hölker, Z. Kolláth, M. O. Gessner, and C. C. Kyba, "Evaluating the summer night sky brightness at a research field site on Lake Stechlin in northeastern Germany," *Journal of Quantitative Spectroscopy and Radiative Transfer*, vol. 181, pp. 24–32, 2016.

[12] M. Nabavi Niaki, N. Saunier, L. Miranda-Moreno, L. Amador Jimenez, and J.-F. Bruneau, "Method for road lighting audit and safety screening at urban intersections," *Transportation Research Record: Journal of the Transportation Research Board*, vol. 2458, pp. 27–36, 12 2014.

[13] M. S. Nabavi Niaki, T. Fu, N. Saunier, L. F. Miranda-Moreno, L. Amador, and J.-F. Bruneau, "Road lighting effects on bicycle and pedestrian accident frequency: Case study in Montreal, Quebec, Canada," *Transportation Research Record*, vol. 2555, no. 1, pp. 86–94, 2016.

[14] J. Armas and J. Laugis, "Increase pedestrian safety by critical crossroads: lighting measurements and analysis," in *European Conference on Power Electronics and Applications*. Aalborg: IEEE, 2007, pp. 1–10.

[15] H. Zhou, F. Pirinccioglu, and P. Hsu, "A new roadway lighting measurement system," *Transportation Research Part C:*

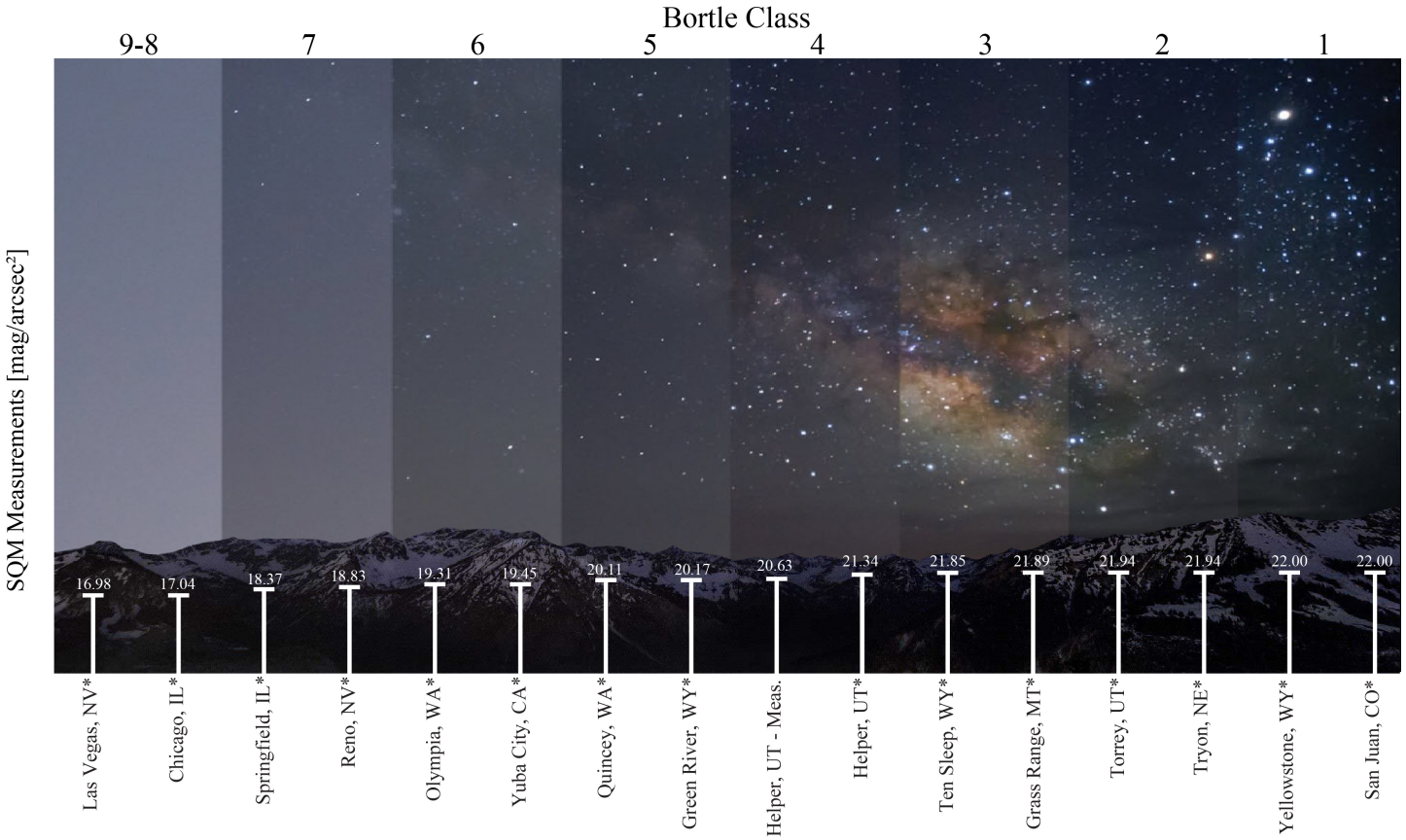

Figure 11: Bortle scale representing night sky brightness and estimated SQM across multiple cities and United States. * Estimated zenith sky brightness data from lightpollutionmap.info [26].

Emerging Technologies, vol. 17, no. 3, pp. 274–284, 2009.

[16] M. Rea, J. Bullough, and Y. Zhou, "A method for assessing the visibility benefits of roadway lighting," *Lighting Research and Technology*, vol. 42, no. 2, pp. 215–241, 2010.

[17] X. He, J. R. Bourne, J. A. Steiner, C. Mortensen, K. C. Hoffman, C. J. Dudley, B. Rogers, D. M. Cropek, and K. K. Leang, "Autonomous chemical-sensing aerial robot for urban/suburban environmental monitoring," *IEEE Systems Journal*, vol. 13, no. 3, pp. 3524–3535, 2019.

[18] M. Schwager, P. Dames, D. Rus, and V. Kumar, "A multi-robot control policy for information gathering in the presence of unknown hazards," in *International Symposium on Robotics Research*, 01 2017, vol. 100, pp. 455–472.

[19] P. M. Dames, M. Schwager, D. Rus, and V. Kumar, "Active magnetic anomaly detection using multiple micro aerial vehicles," *IEEE Robotics and Automation Letters*, vol. 1, no. 1, pp. 153–160, 2015.

[20] J. R. Bourne, M. N. Goodell, X. He, J. Steiner, and K. K. Leang, "Decentralized multi-agent information-theoretic control for target estimation and localization: Finding chemical leaks," *International Journal of Robotics Research (Under review)*, 2020.

[21] G. Yang, J. Liu, C. Zhao, Z. Li, Y. Huang, H. Yu, B. Xu, X. Yang, D. Zhu, X. Zhang *et al.*, "Unmanned aerial vehicle remote sensing for field-based crop phenotyping: current status and perspectives," *Frontiers in Plant Science*, vol. 8, p. 1111, 2017.

[22] K. R. Jenson-Nau, T. Hermans, and K. K. Leang, "Near-optimal area-coverage path planning of energy constrained aerial robots with application in autonomous environmental monitoring," *IEEE Transactions on Automation Science and Engineering (Accepted)*, 2020.

[23] J. A. Steiner, X. He, J. R. Bourne, and K. K. Leang, "Open-sector rapid-reactive collision avoidance: Application in aerial robot navigation through outdoor unstructured environments," *Robotics and Autonomous Systems*, vol. 112, pp. 211–220, 2019.

[24] A. Hänel, T. Posch, S. J. Ribas, M. Aubé, D. Duriscoe, A. Jechow, Z. Kollath, D. E. Lolkema, C. Moore, N. Schmidt *et al.*, "Measuring night sky brightness: methods and challenges," *Journal of Quantitative Spectroscopy and Radiative Transfer*, vol. 205, pp. 278–290, 2018.

[25] "Helper city population estimates," 2019. [Online]. Available: https://www.census.gov/search-results.html?searchType=web\&cssp=SERP\&q=helper\%20population

[26] S. Jurij. Light pollution map. [Online]. Available: https://www.lightpollutionmap.info